

Equation of state of the rigid disk fluid from its triangle distribution

Frank H. Stillinger

Bell Laboratories, Lucent Technologies, Murray Hill, New Jersey 07974 and Princeton Materials Institute, Princeton University, Princeton, New Jersey 08544

Dorothea K. Stillinger

Bell Laboratories, Lucent Technologies, Murray Hill, New Jersey 07974

Salvatore Torquato

Princeton Materials Institute, Princeton University, Princeton, New Jersey 08544 and Department of Chemistry, Princeton University, Princeton, New Jersey 08544

Thomas M. Truskett and Pablo G. Debenedetti

Department of Chemical Engineering, Princeton University, Princeton, New Jersey 08544

(Received 14 July 2000; accepted 12 September 2000)

The distribution function $f^{(3)}$ for triplets of mutual nearest neighbors offers a description of local order for many-particle systems confined to a plane. This paper proposes a self-consistent theory for $f^{(3)}$ in the case of the classical rigid disk model, using three basic identities for closure. Numerical analysis of the resulting coupled nonlinear integral equations yields predictions for the pressure, the boundary tension, and the Kirkwood superposition defect for three disks in mutual contact. The approximation employed implicitly constrains the disk system to remain in the fluid phase at all densities up to close packing ($\rho a^2 = 2/3^{1/2}$). The pressure and boundary tension agree reasonably well with the corresponding predictions of the two-dimensional scaled particle theory, but the former agrees even better with a rational approximant due to Sanchez that reproduces eight virial coefficients. © 2000 American Institute of Physics. [S0021-9606(00)50346-8]

I. INTRODUCTION

The two-dimensional rigid disk system possesses value as a model for planar-surface adsorption phenomena, while offering conceptual simplicity. But in spite of that simplicity it continues to provide substantial challenges to theory, particularly regarding its freezing behavior under lateral compression. It has yet to be conclusively determined whether that freezing transition is a simple first-order phase change in the conventional large-system limit, whether a single higher-order transition is involved, or whether an intervening hexatic phase¹ appears between the isotropic fluid and the triangular crystal. Furthermore, the question of the possible existence of a well-defined metastable extension for the fluid into the compressed density regime beyond freezing constitutes another significant theoretical problem.

The purpose of this presentation is to utilize the distribution function for nearest-neighbor triangles to investigate the fluid-phase equation of state and local order in the classical rigid disk system. As will be seen below, this automatically includes a metastable extension into the high-compression regime. The strategy follows a prior feasibility study² that developed earlier ideas advanced by Collins,^{3,4} and which indicated that given a suitable closure approximation, a self-consistent theory could be constructed for the nearest-neighbor triangle distribution function.

Section II defines the nearest-neighbor triangle distribution function, and reviews the identities it must satisfy, one of which connects to the pressure equation of state.² Section III introduces a generic form for the distribution that provides the basis for a self-consistent closed theory. Numerical

results for this self-consistent theory appear in Sec. IV; these include the pressure, the straight boundary line tension, and the Kirkwood superposition defect for disk triplets in mutual contact. A concluding Sec. V discusses the results obtained as well as opportunities for extending the present approach.

II. TRIANGLE DISTRIBUTION

For any configuration of N disks in a planar region with area A , Voronoi cells can be assigned to each disk by the criterion that all its points lie closer to that disk's center than to any other center. These Voronoi cells are convex polygons that tile the planar region. Any pair of disks whose respective Voronoi cells share a common (linear) boundary constitute a nearest-neighbor pair by convention. The resulting network of nearest-neighbor pair bonds, the Delaunay tessellation, tiles the planar region with nearest-neighbor triangles.^{3,4} Figure 1 illustrates the Voronoi–Delaunay construction.

Let $\rho = N/A$ denote the disk number density. A nearest-neighbor triangle distribution function $f^{(3)}$ can be defined by the requirement that

$$\rho^3 f^{(3)}(\mathbf{r}_1, \mathbf{r}_2, \mathbf{r}_3) d\mathbf{r}_1 d\mathbf{r}_2 d\mathbf{r}_3 \quad (2.1)$$

be the probability that differential area elements $d\mathbf{r}_1$, $d\mathbf{r}_2$, and $d\mathbf{r}_3$ simultaneously contain the centers of three disks that are mutual nearest neighbors. Assuming that periodic boundary conditions apply to A , $f^{(3)}$ must have translation invariance. If the disk system is large and in a fluid phase, rotation and inversion symmetries must also apply to $f^{(3)}$.²

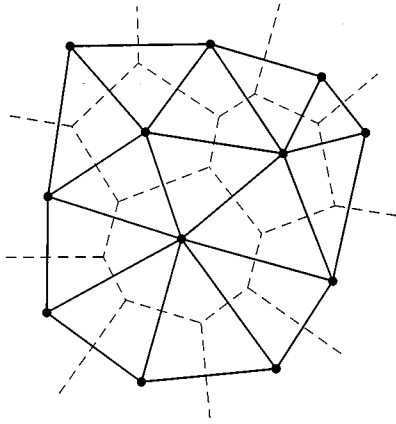


FIG. 1. The Voronoi–Delaunay construction in the plane. Particle center positions have been indicated as small dark circles, their respective Voronoi cells have been outlined by dotted lines, and nearest-neighbor pairs have been connected by solid lines.

Two obvious integral conditions must be obeyed by $f^{(3)}$ for any two-dimensional many-particle system. The first is that the number of nearest neighbor triangles is exactly $2N$,

$$2N = (\rho^3/3!) \int d\mathbf{r}_1 \int d\mathbf{r}_2 \int d\mathbf{r}_3 f^{(3)}. \quad (2.2)$$

The second is that the sum of all triangle areas Δ must total A ,²

$$A = (\rho^3/3!) \int d\mathbf{r}_1 \int d\mathbf{r}_2 \int d\mathbf{r}_3 \Delta f^{(3)}. \quad (2.3)$$

The spatial integrations in these last two equations cover area A , and the denominator factors $3!$ compensate for overcounting.

On account of the symmetries involved, it is convenient to use triangle side lengths r, s, t as spatial variables for $f^{(3)}$. These lengths are subject to the triangle inequalities, and only determine the shape of a triangle to within an inversion operation. Taking these features into account, and making the replacement²

$$d\mathbf{r}_1 d\mathbf{r}_2 d\mathbf{r}_3 \rightarrow 8\pi A r s t [M(r, s, t)]^{-1/2} dr ds dt, \quad (2.4)$$

where

$$M(r, s, t) = 2(r^2 s^2 + r^2 t^2 + s^2 t^2) - r^4 - s^4 - t^4 \\ = (r + s + t)(-r + s + t)(r - s + t)(r + s - t), \quad (2.5)$$

the transformed integrations become restricted to the region $M > 0$. Consequently Eq. (2.2) yields the following condition:

$$3/(2\pi\rho^2) = \int dr \int ds \int dt r s t [M(r, s, t)]^{-1/2} f^{(3)}(r, s, t). \quad (2.6)$$

Furthermore the expression for triangle area in terms of r, s, t is simply

$$\Delta(r, s, t) = (1/4)[M(r, s, t)]^{-1/2}, \quad (2.7)$$

so that Eq. (2.3) leads to the second condition,

$$3/(\pi\rho^3) = \int dr \int ds \int dt r s t f^{(3)}(r, s, t). \quad (2.8)$$

For the special case of the rigid disk system, $f^{(3)}$ necessarily vanishes if any one of r, s, t is less than a , the distance of closest disk approach. From the geometry of disk exclusion, any three disks that are sufficiently close to one another are necessarily nearest neighbors. In particular this is true at mutual contact, with r, s , and t all equal to a . As a result $f^{(3)}$ must equal the conventional triplet correlation function $g^{(3)}$ for this configuration,

$$f^{(3)}(a, a, a) = g^{(3)}(a, a, a). \quad (2.9)$$

The virial equation of state for virial pressure p involves $g^{(2)}(a)$, the contact pair correlation function,⁵

$$\beta p = \rho + (\pi/2)\rho^2 a^2 g^{(2)}(a), \quad \beta = 1/k_B T. \quad (2.10)$$

In analogy to Eq. (2.9) above, $g^{(2)}(a)$ is identical to $f^{(2)}(a)$, the contact value of the nearest-neighbor pair distribution function. Because $f^{(2)}(r)$ can be extracted from $f^{(3)}(r, s, t)$ by integrating over two triangle sides, it is possible to derive a third integral condition on $f^{(3)}$, specifically for the disk system, that relates it to the pressure,²

$$\frac{1}{\pi\rho^2 a^2} \left(\frac{\beta p}{\rho} - 1 \right) = \int ds \int dt s t [M(a, s, t)]^{-1/2} f^{(3)}(a, s, t). \quad (2.11)$$

For later use it is relevant to mention that closed-form approximations are available for the disk fluid equation of state. One of the simplest of these emerges from the two-dimensional version of the scaled-particle theory,⁶

$$\beta p a^2 = \rho a^2 [1 - (\pi\rho a^2/4)]^{-2}. \quad (2.12)$$

A more complicated form due to Sanchez,⁷ a ratio of polynomials in density that reproduces eight virial coefficients, has the following form:

$$\beta p a^2 = \rho a^2 P(\rho a^2)/Q(\rho a^2); \quad (2.13)$$

$$P(x) = 1 + 0.816\,508x - 0.294\,1438x^2 + 0.146\,136x^3; \quad (2.14)$$

$$Q(x) = 1 - 0.754\,296x - 1.038\,819x^2 \\ + 1.170\,521x^3 - 0.308\,969x^4. \quad (2.15)$$

III. SELF-CONSISTENT APPROXIMATION

The radius R of the circumscribed circle for a triangle with sides r, s, t possesses the following functional form:

$$R(r, s, t) = r s t [M(r, s, t)]^{-1/2}. \quad (3.1)$$

In order that three particle centers in such a triangular arrangement be mutual nearest neighbors it is necessary and sufficient that no other particle center lie within the triangle's circumscribed circle.^{2,3} This circumscribed circle forms only part of the excluded zone for the rigid disk case however, since the disk repulsions themselves add three circular caps of radius a centered at the three particles involved. The Appendix supplies an explicit form for $X(r, s, t)$, the area of this composite excluded region for any disk triplet of mutual

nearest neighbors. The Appendix also provides an explicit expression for $L(r,s,t)$, the length of the boundary of $X(r,s,t)$.

The distribution function $f^{(3)}$ in principle can be expressed as a suitably normalized Boltzmann factor for the reversible work W that must be expended to create the excluded region X ,

$$f^{(3)}(r,s,t) = C \exp[-\beta W(r,s,t)]. \quad (3.2)$$

Following the strategy used to advantage by the scaled particle theory,⁶ W will now be approximated as a sum of pressure-area work and line tension-boundary length work,

$$f^{(3)} \cong C \exp[-\beta p X(r,s,t) - \beta \gamma L(r,s,t)]; \quad (3.3)$$

here γ is the appropriate line tension. This expression contains three unknown scalars, C , p , and γ , which exact conditions (2.6), (2.8), and (2.11) are available to determine self-consistently. Section IV presents the results of a numerical analysis of these three simultaneous integral equations.

Our earlier feasibility study² was designed in part to demonstrate that self-consistent solutions were indeed possible with this kind of statistical-geometric approach. That work invoked a crude, minimal approximation in which X and L were replaced merely by the circumscribed circle area and perimeter, respectively, an approach that is asymptotically correct in the low density limit. The minimal approximation appeared to yield unique numerical solutions that were qualitatively correct for the fluid phase over the entire density range from dilute to crystalline close-packed, thereby providing motivation for the more detailed and accurate analysis of the present paper.

IV. NUMERICAL RESULTS

The three simultaneous equations that result from substituting $f^{(3)}$ approximation (3.3) into conditions (2.6), (2.8), and (2.11) have been solved numerically using the Levenberg–Marquardt algorithm implemented in a commercial software package.⁸ The density range considered was

$$0.20 \leq \rho a^2 \leq 1.05 \quad (4.1)$$

(crystal close-packing occurs at $\rho a^2 = 2/3^{1/2} = 1.1547\dots$). The form (3.3) assumed for $f^{(3)}$ becomes asymptotically correct in the low density limit, where $\beta\gamma$ vanishes, and βp obeys the ideal gas law.² Consequently, extending the lower limit in Eq. (4.1) closer to zero had no intrinsic interest. Also, calculations beyond the upper density limit shown ran the risk of accumulating substantial errors due to the large magnitudes and the rapid spatial variations of the various quantities involved. Only a single solution emerged over the density range investigated; a systematic search failed to uncover an alternate branch that could be identified as belonging to a crystalline phase.

Table I shows values of the dimensionless pressure $\beta p a^2$ that emerge from the numerical analysis. Corresponding results from the scaled particle theory, Eq. (2.12), and from the Sanchez rational approximant, Eq. (2.13), have also been included in Table I for comparison. None of the three

TABLE I. Dimensionless pressures $\beta p a^2$ for the self-consistent calculations based on Eq. (3.3). For comparison, corresponding results are shown for the scaled particle theory (SPT), Eq. (2.12), and for the Sanchez rational approximant (SA), Eq. (2.13).

ρa^2	$\beta p a^2$	$\beta p a^2(\text{SPT})$	$\beta p a^2(\text{SA})$
0.20	0.281	0.281	0.282
0.25	0.388	0.387	0.389
0.30	0.516	0.513	0.517
0.35	0.671	0.666	0.672
0.40	0.859	0.850	0.861
0.45	1.089	1.076	1.092
0.50	1.376	1.356	1.380
0.55	1.736	1.705	1.741
0.60	2.191	2.146	2.199
0.65	2.777	2.713	2.789
0.70	3.547	3.453	3.563
0.75	4.569	4.441	4.599
0.80	5.968	5.791	6.024
0.85	7.932	7.692	8.052
0.90	10.781	10.473	11.074
0.95	15.149	14.740	15.886
1.00	22.237	21.714	24.380
1.05	35.407	34.156	42.391
$2/3^{1/2}$	$+\infty$	133.219	-636.636

exhibit a freezing transition, which a variety of computer simulations predicts to occur over the approximate density range,⁹

$$0.88 \leq \rho a^2 \leq 0.91. \quad (4.2)$$

Thus, all three pressure columns in Table I represent fluid phases with metastable extensions into the overcompressed regime. Note that the results of the present approach lie between the predictions of the scaled particle theory and the Sanchez rational approximant, though significantly closer to the latter than to the former over most of the density range.

Table II reports values obtained for $\beta\gamma a$, the dimension-

TABLE II. Numerically computed values of the line tension $\beta\gamma a$, along with the predictions of the rigid-disk scaled particle theory (SPT), Eq. (4.3).

ρa^2	$\beta\gamma a$	$\beta\gamma a(\text{SPT})$
0.20	-0.024	-0.022
0.25	-0.034	-0.038
0.30	-0.053	-0.060
0.35	-0.081	-0.091
0.40	-0.120	-0.134
0.45	-0.174	-0.190
0.50	-0.246	-0.266
0.55	-0.346	-0.368
0.60	-0.483	-0.506
0.65	-0.674	-0.692
0.70	-0.944	-0.949
0.75	-1.323	-1.308
0.80	-1.878	-1.819
0.85	-2.701	-2.568
0.90	-3.960	-3.702
0.95	-5.973	-5.499
1.00	-9.359	-8.527
1.05	-15.904	-14.084
$2/3^{1/2}$	$-\infty$	-60.408

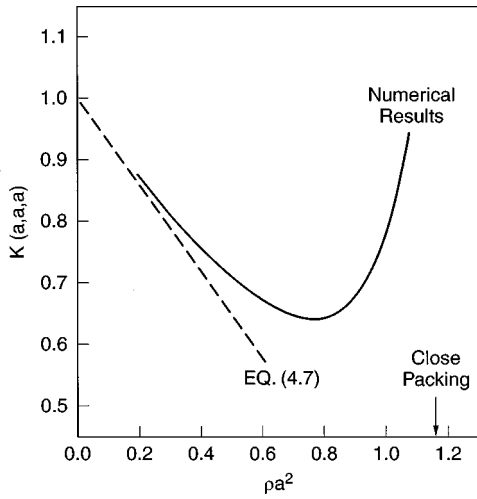


FIG. 2. Calculated values of the Kirkwood superposition defect function, Eq. (4.4), for disk triplets in mutual contact.

less line tension. Scaled particle theory for rigid disks also provides an explicit prediction for this quantity,⁶

$$\beta\gamma a = -\frac{2}{\pi} \left(\frac{\pi\rho a^2/4}{1-\pi\rho a^2/4} \right)^2. \quad (4.3)$$

That both approaches yield negative results for $\beta\gamma a$ implies that disks in the fluid phase tend to cluster at a rigid boundary, specifically that of length $L(r,s,t)$ surrounding $X(r,s,t)$, suggesting that “tension” would more accurately be termed “elongation tendency” in the present context.

The Kirkwood superposition approximation^{10,11} applied at the particle triplet level assumes that $g^{(3)}(r,s,t)$ can be replaced by the product of the three pair correlation functions $g^{(2)}$, i.e., it supposes that the ratio

$$K(r,s,t) = g^{(3)}(r,s,t)/g^{(2)}(r)g^{(2)}(s)g^{(2)}(t) \quad (4.4)$$

is identically unity. In fact, a Mayer cluster expansion reveals that this Kirkwood superposition defect function K deviates from unity in the low density regime by an $O(\rho^2)$ correction,¹²

$$K(r_{12},r_{13},r_{23}) = 1 + \rho \int d\mathbf{r}_4 f_M(r_{14})f_M(r_{24})f_M(r_{34}) + O(\rho^2), \quad (4.5)$$

where

$$f_M(r_{ij}) = \exp[-\beta v(r_{ij})] - 1 \quad (4.6)$$

is the Mayer function for pair potential v . Equations (2.9) and (2.10) above show that the Kirkwood superposition defect for three disks in mutual contact, $K(a,a,a)$, can be extracted as a natural by-product of the numerical study. Figure 2 shows a plot of this quantity over the density range (4.1). This Fig. 2 also includes the low-density linear estimate from Eq. (4.5),

$$K(a,a,a) \cong 1 - 0.7048\rho a^2 + O(\rho^2). \quad (4.7)$$

The graph shows that the predicted $K(a,a,a)$ passes through a minimum less than unity when $\rho a^2 \cong 0.77$, but rises at

higher density to show closer agreement with the Kirkwood superposition approximation, particularly in the metastable overcompressed range.

V. DISCUSSION

Although the scaled particle theory offers an appealing and useful approximation for the rigid disk fluid phase,⁶ it suffers from an obvious shortcoming. Specifically it predicts a finite pressure at and somewhat beyond the close-packed density $\rho_0 a^2 = 1.1547\dots$, only diverging at the geometrically unattainable higher density $\rho_{SPT} a^2 = 1.2732\dots$. Furthermore, as Eq. (2.12) above reveals, the pressure divergence of the scaled particle theory is a second-order pole, whereas basic dimensional arguments stemming from the multidimensional geometry of available configuration space require a simple-pole divergence,¹³

$$\begin{aligned} \beta p a^2 &= \sigma/(1-\rho/\rho_0) + O(1), \\ \sigma &= 4/3^{1/2} = 2.3094\dots \end{aligned} \quad (5.1)$$

The Sanchez approximant (2.13) possesses a simple-pole divergence at a density ρ_{SA} only slightly less than that at crystalline close packing,

$$\rho_{SA} \cong 1.146197; \quad (5.2)$$

however the residue at this pole is rather large compared to the expected value shown in Eq. (5.1),

$$(\beta p a^2)_{SA} \cong 4.5822/(1-\rho/\rho_{SA}) + O(1). \quad (5.3)$$

By adapting a previous analysis of the high-compression limit² to the present self-consistent approximation, one finds that the pressure divergence correctly occurs at ρ_0 as a simple pole, but with a somewhat magnified residue,

$$\beta p a^2 = 1.5\sigma/(1-\rho/\rho_0) + O(1). \quad (5.4)$$

Evidently the $f^{(3)}$ approximation used in the present self-consistent theory implicitly inhibits crystal nucleation. Yet it permits the metastable fluid phase to approach arbitrarily close to the crystalline close-packing density $\rho_0 a^2$, and in that limit all nearest-neighbor disk triangles are forced into compact equilateral form, just as in the perfect triangular lattice. The apparent explanation is that the approximation used effectively enforces a size limitation for local crystalline arrangements of disks, but that this size increases continuously to infinity as ρ approaches ρ_0 . This constraint is sufficient to inhibit a discrete freezing transition, but permits the metastable fluid to transform continuously under compression ultimately to the well-ordered crystal.

The fact that approximation (3.3) for the basic quantity $f^{(3)}$ constrains the system to remain in a single fluid phase at all possible densities raises some important issues for future consideration. One obviously is what modification of form (3.3) would be required to describe the freezing transition, and to reproduce the correct pole residue, Eq. (5.1), for the pressure of the ordered crystal. Another issue concerns the values that the present self-consistent approximation assigns to the disk model virial coefficients, and how they compare with known exact values.⁷ It would also be useful to investigate whether a straightforward extension of the present ap-

proach for the disk fluid could be constructed for more realistic interactions, e.g., the Lennard-Jones pair potential.

The corresponding treatment for rigid spheres in three dimensions would involve a distribution function $f^{(4)}$ for nearest-neighbor tetrahedra. As briefly discussed in our earlier paper² the generalization is conceptually straightforward but technically difficult. Unlike the case of compact triangles in the plane, compact tetrahedra alone cannot tile three-dimensional space. Nevertheless, adapting the present approach to the rigid sphere model would be a desirable advance, particularly in connection with the continuing interest in the definition and properties of irregular sphere packings.¹⁴

ACKNOWLEDGMENTS

S.T. gratefully acknowledges the support of the U.S. Department of Energy, Office of Basic Energy Sciences (Grant No. DE-FG02-92ER14275). T.M.T. acknowledges the National Science Foundation for financial support. P.G.D. gratefully acknowledges support of the U.S. Department of Energy, Office of Basic Energy Science (Grant No. DE-FG02-87ER13714).

APPENDIX

Expressions for the excluded area X and the boundary length L of that area, for an arbitrary configuration r, s, t of three nearest-neighbor disks, can be derived by straightforward means that need not be reproduced here. The form of the results depends upon which of the three disk pairs, if any, have radius- a circular caps that overlap outside the radius- R circumscribed circle of disk centers. This overlap criterion depends on comparison of each pair separation r, s , and t with the following distance:

$$d(R) = 2a \left(1 - \frac{a^2}{4R^2} \right)^{1/2}. \quad (\text{A1})$$

Equation (3.1) provides the explicit form for $R(r, s, t)$

The excluded area is found to be

$$X(r, s, t) = \pi R^2 + F(r, R) + F(s, R) + F(t, R), \quad (\text{A2})$$

where ($\text{asn} \equiv \text{arc sin}$, $\text{acs} \equiv \text{arc cos}$),

$$F(u, R) = a^2 \text{asn} \left(\frac{u}{2a} \right) + (a^2 - R^2) \text{asn} \left(\frac{u}{2R} \right) + (uR/2) \left[\left(1 - \frac{u^2}{4R^2} \right)^{1/2} + \left(\frac{a^2}{R^2} - \frac{u^2}{4R^2} \right)^{1/2} \right],$$

$$[a \leq u \leq d(R)];$$

$$= a^2 \text{acs} \left(\frac{a}{2R} \right) + (a^2 - R^2) \text{acs} \left(1 - \frac{a^2}{2R^2} \right) + aR \left(1 - \frac{a^2}{4R^2} \right)^{1/2}, \quad [d(R) \leq u]. \quad (\text{A3})$$

The corresponding expressions for the boundary area are

$$L(r, s, t) = 2\pi R + G(r, R) + G(s, R) + G(t, R), \quad (\text{A4})$$

where

$$G(u, R) = -2R \text{asn} \left(\frac{u}{2R} \right) + (2a) \text{acs} \left[\left(1 - \frac{u^2}{4R^2} \right)^{1/2} \times \left(1 - \frac{u^2}{4a^2} \right)^{1/2} - \frac{u^2}{4aR} \right], \quad [a \leq u \leq d(R)];$$

$$= \pi a + (a - 2R) \text{acs} \left(1 - \frac{a^2}{4R^2} \right), \quad [d(R) \leq u]. \quad (\text{A5})$$

As a result of the disk repulsions, the overlap regions for pairs of circular caps remain separate.

- ¹J. M. Kosterlitz and D. J. Thouless, *J. Phys. C* **6**, 1181 (1973); B. I. Halperin and D. R. Nelson, *Phys. Rev. Lett.* **41**, 121 (1978); A. P. Young, *Phys. Rev. B* **19**, 1855 (1979).
- ²D. K. Stillinger, F. H. Stillinger, S. Torquato, T. M. Truskett, and P. G. Debenedetti, *J. Stat. Phys.* **100**, 49 (2000).
- ³R. Collins, *J. Phys. C* **1**, 1461 (1968).
- ⁴R. Collins, in *Phase Transitions and Critical Phenomena*, edited by C. Domb and M. S. Green (Academic, New York, 1972), Vol. 2, pp. 271–303.
- ⁵H. L. Frisch, *Adv. Chem. Phys.* **IV**, 229 (1964).
- ⁶E. Helfand, H. L. Frisch, and J. L. Lebowitz, *J. Chem. Phys.* **34**, 1037 (1961).
- ⁷I. C. Sanchez, *J. Chem. Phys.* **101**, 7003 (1994), Eq. (11).
- ⁸MATHCAD, version 8.0, Mathsoft Corp., Cambridge, MA.
- ⁹A. C. Mitus, H. Weber, and D. Marx, *Phys. Rev. E* **55**, 6855 (1997); references therein review the major simulation results for disks.
- ¹⁰J. G. Kirkwood and E. M. Boggs, *J. Chem. Phys.* **10**, 394 (1942).
- ¹¹T. L. Hill, *Statistical Mechanics* (McGraw-Hill, New York, 1956), pp. 195–198.
- ¹²S. A. Rice and P. Gray, *The Statistical Mechanics of Simple Liquids* (Wiley-Interscience, New York, 1965), p. 85.
- ¹³F. H. Stillinger and Z. W. Salsburg, *J. Stat. Phys.* **1**, 179 (1969).
- ¹⁴S. Torquato, T. M. Truskett, and P. G. Debenedetti, *Phys. Rev. Lett.* **84**, 2064 (2000).